European Journal of Radiology Open 13 (2024) 100592

Contents lists available at ScienceDirect

European Journal of Radiology Open

journal homepage: www.elsevier.com/locate/ejro

MRI-based machine learning radiomics for prediction of HER2 expression status in breast invasive ductal carcinoma

Hong-Jian Luo [a], Jia-Liang Ren [b], Li mei Guo [c], Jin liang Niu [c], Xiao-Li Song [c,*]

[a] Department of Radiology, The Third Affiliated Hospital of Zunyi Medical University (The First People's Hospital of Zunyi), Zuiyi, Guizhou province, China
[b] GE HealthCare, Beijing, China
[c] Department of Radiology, Second Hospital of Shanxi Medical University, Taiyuan, Shanxi province, China

HIGHLIGHTS

- A 3-tier structure consisting of HER2-positive, HER2-low, and HER2-zero could more effectively fit clinical needs for IDC.
- Multisequence MRI-based machine learning radiomics showed good efficiency in classifying expression status of HER2.
- Random forest algorithm exhibits higher diagnostic performance than the classification algorithms of LR and SVM.

ARTICLE INFO

Keywords:
Magnetic Resonance Imaging
Invasive Ductal Breast Carcinoma
Human Epidermal Growth Factor Receptor 2
Radiomics
Machine learning

ABSTRACT

Background: Human epidermal growth factor receptor 2 (HER2) is a tumor biomarker with significant prognostic and therapeutic implications for invasive ductal breast carcinoma (IDC).
Objective: This study aimed to explore the effectiveness of a multisequence magnetic resonance imaging (MRI)-based machine learning radiomics model in classifying the expression status of HER2, including HER2-positive, HER2-low, and HER2 completely negative (HER2-zero), among patients with IDC.
Methods: A total of 402 female patients with IDC confirmed through surgical pathology were enrolled and subsequently divided into a training group (n = 250, center I) and a validation group (n = 152, center II). Radiomics features were extracted from the preoperative MRI. A simulated annealing algorithm was used for key feature selection. Two classification tasks were performed: task 1, the classification of HER2-positive vs. HER2-negative (HER2-low and HER2-zero), and task 2, the classification of HER2-low vs. HER2-zero. Logistic regression, random forest (RF), and support vector machine were conducted to establish radiomics models. The performance of the models was evaluated using the area under the curve (AUC) of the operating characteristics (ROC).
Results: In total, 4506 radiomics features were extracted from multisequence MRI. A radiomics model for prediction of expression state of HER2 was successfully developed. Among the three classification algorithms, RF achieved the highest performance in classifying HER2-positive from HER2-negative and HER2-low from HER2-zero, with AUC values of 0.777 and 0.731, respectively.
Conclusions: Machine learning-based MRI radiomics may aid in the non-invasive prediction of the different expression status of HER2 in IDC.

1. Introduction

Breast carcinoma is the most prevalent cancer and the leading cause of cancer-related mortality in women worldwide [1]. Invasive ductal carcinoma (IDC), which accounts for 80 % of all invasive breast cancers, is a heterogeneous group of diseases with different characteristics and behaviors. Human epidermal growth factor receptor 2 (HER2) protein serves as a tumor biomarker with significant prognostic and therapeutic implications in invasive breast carcinoma [2]. Historically, HER2 status has typically been classified as either HER2-positive (immunohistochemical [IHC] score of 3+, or amplification detected through HER2 gene fluorescence in-situ hybridization [FISH]) or HER2-negative. This

* Corresponding author.
E-mail address: songxiaoli99@126.com (X.-L. Song).

https://doi.org/10.1016/j.ejro.2024.100592
Received 18 April 2024; Received in revised form 8 July 2024; Accepted 14 July 2024
Available online 19 July 2024

binary categorization plays a crucial role in determining the prognosis and treatment decisions for breast carcinoma [3]. HER2-positive invasive breast cancer is characterized by high invasiveness, high degree of malignancy, recurrence, metastasis, and poor prognosis [4]. Anti-HER2 targeted treatment is routinely considered in the management of the breast carcinomas that test positive for HER2 in clinical practice [5]. Therefore, it is crucial to accurately evaluate the HER2 status in individuals with invasive breast carcinomas. Recently, there has been growing attention in invasive breast carcinomas regarding a newly proposed category known as "HER2-low" (IHC score of 1+, or 2+ with FISH-negative). Approximately half of breast tumors that are categorized as HER2-negative display HER2-low expression [6]. Compared to both completely HER2--negative (HER2--zero [IHC score of 0]) and HER2-positive, the HER2-low breast carcinomas exhibit unique characteristics in terms of biology, clinicopathological features, therapeutic response, and clinical outcome [7]. In HER2-low breast carcinoma, recent reports have shown encouraging response rates of antibody-drug conjugates, trastuzumab-emtansine and trastuzumab-deruxtecan (formerly DS8201a) [8–10]. Hence, it is imperative to identify the HER2-low status as a novel classification of breast carcinoma. In invasive breast carcinoma, a three-tier structure consisting of HER2-positive, HER2-low, and HER2-zero can more effectively meet the clinical needs to enhance prognosis prediction and provide personalized treatment guidance.

The HER2 status is primarily determined through IHC and FISH examination after biopsy or surgical tumor excision. Nevertheless, biopsy procedures are associated with complications. Furthermore, the smaller sample size obtained from the core needle biopsy procedure may not be sufficient to represent the HER2 status of the whole tumor owing to the intratumor heterogeneity of HER2 expression [11]. Moreover, the instability of HER2 expression is evident throughout the progression from initial to relapsed breast cancer [12]. Therefore, a non-invasive, economical and effcetive method is required for the pretreatment prediction of HER2 status in IDC.

In clinical practice, the magnetic resonance imaging (MRI) has become a routine examination for patients at a risk of breast carcinoma. Nonetheless, MRI still presents limitations in the evaluation of HER2 status. Radiomics is a novel research field focused on extracting and analyzing imaging features to reflect tissue information [13]. It has been used to identify molecular subtypes, predict responses to neoadjuvant chemotherapy, and forecast survival outcomes in breast carcinoma [14–17]. According to recent studies, radiomics derived from MRI can potentially offer insights into forecasting the HER2 status in breast carcinomas [18,19]. However, these investigations anticipated the HER2 condition by utilizing a binary classification, merging HER2-low and HER2-zero as HER2-negative. In this study, we aimed to use multisequence MRI-based radiomic features coupled with machine learning to classify the various expression statuses of HER2 in IDC.

2. Materials and methods

2.1. Patients

A total of 402 patients, 250 from center I and 152 from center II, were enrolled in this retrospective multicenter study. The inclusion criteria were as follows: (1) confirmed IDC through surgical pathology; and (2) underwent MRI less than 1 month before surgery. The exclusion criteria were as follow: (1) preoperative treatment, (2) lack of complete pathology data (HER-2 status unknown), (3) inability to visualize a known malignancy, and (4) poor MRI quality. Data from centers I and II were assigned to the training and validation cohorts, respectively. Clinical characteristics, including age, body mass index, maximum axial diameter of the tumor size, type of time-intensity curve (TIC), estrogen receptor (ER), progesterone receptor (PR), and Ki-67, were extracted from the patients' medical records. The TIC were divided into type I (inflow type), type II (plateau type), and type III (outflow type). Patients were classified into three subtypes based on their HER2 expression status: HER2-positive, HER2-low, and HER2-zero. Two binary classification tasks were conducted, involving the categorization of HER2 as either positive or negative (including HER2-low and HER2-zero) in task 1 and the classification of HER2-low from HER2-zero in task 2. A flowchart of the study is shown in Fig. 1. The institutional review boards of both participating centers approved this retrospective study and waived the requirement for informed consent.

2.2. MRI acquisition and image analysis

All patients underwent preoperative breast MRI scan. Axial fat saturation T2 weighted image (FST2WI) was acquired before contrast medium administration. Next, the DCE-MRI series were obtained prior to and at five to six points at 60 sec intervals using contrast medium (gadodiamide and gadopentetate dimeglumine) at a dose of 0.1 mmol/kg and a rate of 2–3 ml/s. The first phase (T1WI) and peak enhanced phase (T1WI+C), according to the TIC, were selected for analysis. Details of the MR images acquisition parameters can be found in the Supplementary Material S1. A radiologist manually delineated the three-dimensional region of interest (ROI) covering the entire tumor volume using ITK-SNAP 3.8.0 software on axial FST2WI, T1WI, and T1WI+C (Fig. 2). Subsequently, 50 cases were randomly selected, and segmentation was repeated by another radiologist.

2.3. Histopathological analysis

The immunohistochemical status of the IDCs, including ER, PR, Ki-67, and HER2 status, were obtained from the final histopathological results of the surgical tumor specimens. ER and PR with over 1 % staining were defined as hormone receptor (HR)-positive [20]. The cutoff value for Ki-67 was set at 30 % [21]. HER2 status was categorized as HER2-positive (IHC score of 3+ and 2+ with FISH-positive), HER2-low (IHC score of 1+, or 2+ with FISH-negative), and HER2 -negative (IHC score of 0) (Fig. 3).

2.4. Radiomics feature extraction

Prior to image extraction, the pixels of the image were resampled using B-spline interpolation to a uniform voxel size of $1 \times 1 \times 1$ mm. Subsequently, gray-level normalization was performed using the z-score method, with pixel intensity values constrained to within ± 3 standard deviations of the mean. Additionally, gray levels were discretized using bin widths of 5. A series of image filters were then used, including the Laplacian of Gaussian, gradient, local binary pattern, and wavelet image filters. The PyRadiomics package was used to extract features from the original and filtered images [22]. The process of features extraction and standardization followed the Image Biomarker Standardization Initiative guidelines [23]. Supplementary Material S2 presents the detailed information regarding these features. In total, 1502 features were acquired for each sequence, including 14 shape, 288 first-order, and 1200 texture features.

2.5. Radiomics selection and model establishment

Initially, the ComBat harmonization technique was applied to align the feature distributions computed from various MRI scanners and protocols. Subsequently, the intraclass correlation coefficient (ICC) was utilized to evaluate the interobserver variability of the radiomics features. Features with an ICC greater than 0.75 were retained for further analysis. Subsequently, univariable analysis was conducted to identify significant features using the Wilcoxon rank-sum test ($P < 0.05$). The Boruta algorithm was employed to remove irrelevant features [24]. Finally, the best radiomics features were selected using simulated annealing (SA) algorithm. This algorithm considers spectral characteristics from a global view of the data and extracts features in an optimized

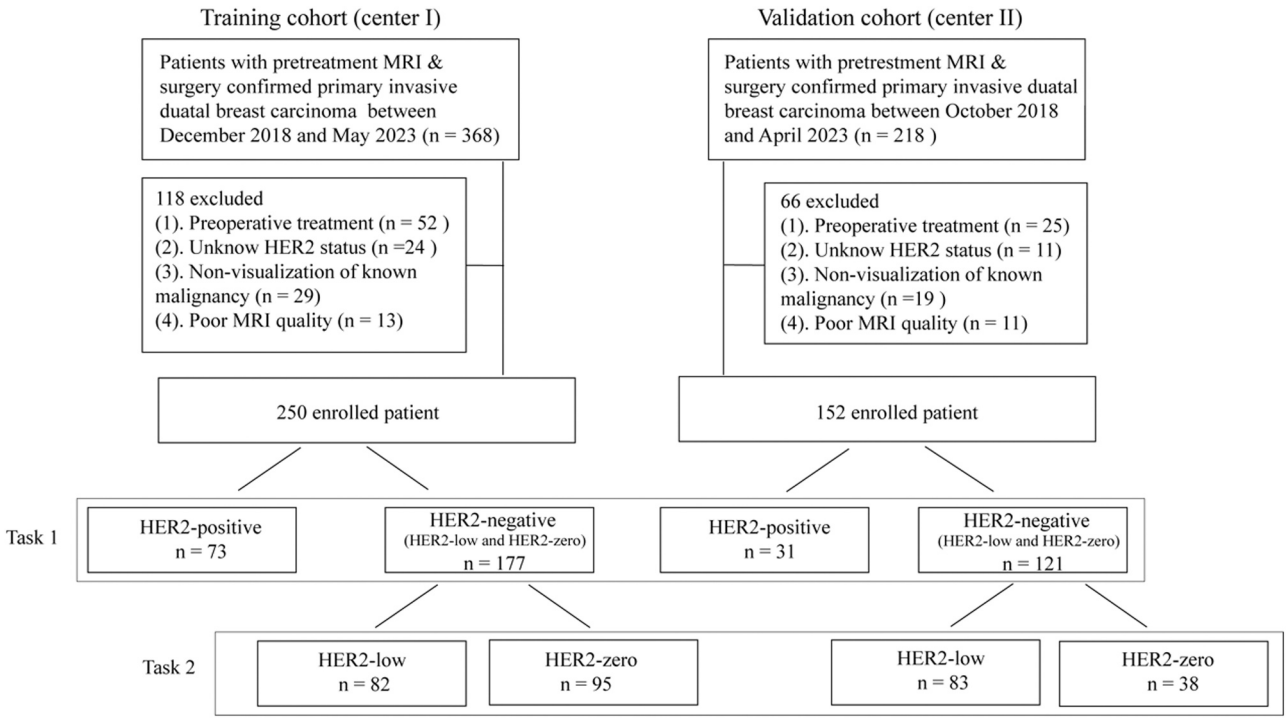

Fig. 1. Flowchart of patient selection and study design.

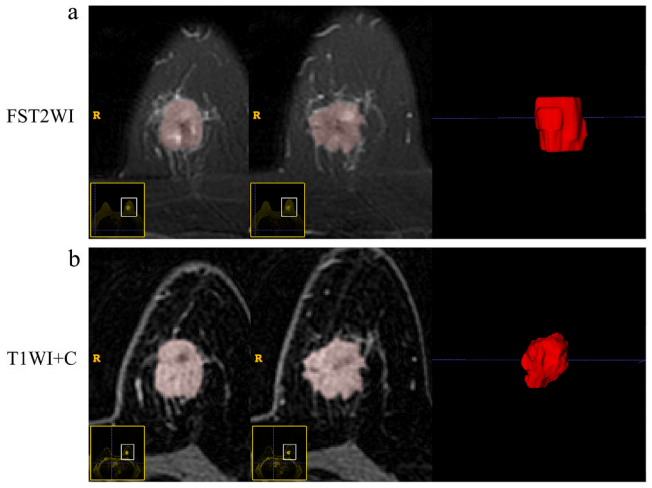

Fig. 2. Examples of manual lesion segmentation in a patient with endometrial cancer. Axial fat saturation T2-weighted imaging (FST2WI) with manually segmented regions of IDC (a) and axial contrast-enhanced T1-weighted imaging (T1WI+C) (b).

combination to avoid overfitting the model training [25].

Radiomics models were established to identify the HER2 status based on the retained radiomics features. Two classification tasks were conducted. The first step involved establishing a model to distinguish between HER2-positive and HER2-negative (including HER2-low and HER2-zero). Next, the task 2 was executed to further classify HER2-low and HER2-zero. Three machine learning algorithms—logistic regression (LR), random forest (RF), and support vector machine (SVM)—, were utilized to build the prediction models. These models were developed using the training cohort and subsequently validated on both the training and validation cohorts.

2.6. Statistical analysis

R software (version 4.1.0, www.rproject.org) was used to perform statistical analyses. The Mann-Whitney *U* test and chi-square test were used to compare the variations in variables. Receiver operating characteristic (ROC) curves were plotted. The area under the ROC curve (AUC), accuracy, sensitivity, and specificity were used to evaluate the models' performance. Youden's index was utilized to determine the optimal cutoff point on the ROC curve. The DeLong test was employed to compare the differences in values between the radiomics models. The clinical usefulness of the models was evaluated through decision curve analysis (DCA). Statistical significance was set at $P < 0.05$.

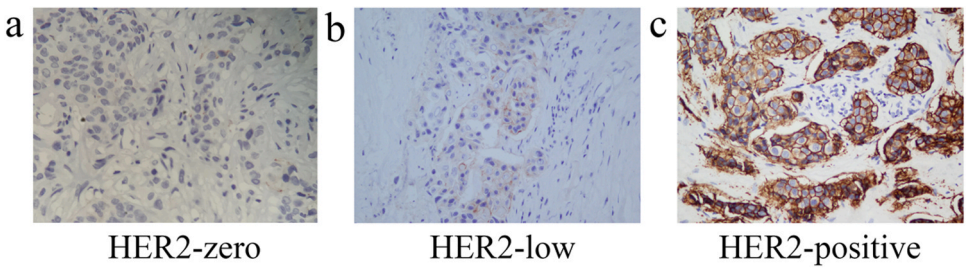

Fig. 3. Immunohistochemistry (IHC) showing an invasive ductal breast carcinoma (IDC) with completely negative expression of human epidermal growth factor receptor 2 (HER2) (HER2-zero) (a), an IDC with HER2-low (b), and IDC with HER2-positive (all original magnification ×40).

3. Results

3.1. Patient clinical characteristics

In total, 402 female patients with IDC were consecutively enrolled and stratified into the training (250 patients, center I), and validation (152 patients, center II) cohorts. Table 1 presents the clinical characteristics of the training and validation cohorts. The HER2-positive, HER2-low, and HER2-zero proportions were 29.20 %, 32.80 %, and 38.00 %, respectively, in the training, and 20.39 %, 54.61 %, and 25.00 %, respectively, in validation cohort.

3.2. Feature selection and model establishment

From the multisequence MRI, 4506 radiomic features were extracted. ComBat eliminated the radiomics features variations caused by intrascanner variability. For task 1, 26 features were retained after the ICC and univariate analyses. After the Boruta algorithm selection, 12 radiomics features were selected. Finally, four radiomics features remained after the SA algorithm was applied, including three from FST2WI (original_GLRLM_RunEntropy, wavelet.LHL_GLCM_Difference Variance, and wavelet.LHL_GLCM_DifferenceVariance), and one from T1WI+C (wavelet.LHH_GLRLM_LowGrayLevelRunEmphasis). For task 2, four radiomics features finally remained with three from FST2WI (original_GLSZM_GrayLevelNonUniformityNormalized, wavelet.LLL_GLRLM_GrayLevelNonUniformityNormalized, and wavelet.LLL_GLSZM_GrayLevelNonUniformityNormalized) and one from T1WI+C (wavelet.LHH_GLCM_ClusterShadewere). The distribution of radiomics features is shown in Supplementary Material S3. Three machine learning classifiers, LR, RF, and SVM, were used to establish the prediction models in the training and validation cohorts.

Table 1
Patient clinical characteristics in the training and validation cohorts [median (Q1, Q3) or no. (%)].

	Training cohort (n = 250)	Validation cohort (n = 152)	*P*
Age (year)	49.00 [44.00;56.00]	50.00 [45.000;57.000]	0.637
Body mass index (kg/cm^2)	24.10 [22.13;26.60]	23.93 [22.20;26.67]	0.956
Tumor size (cm)	2.50 [1.90;3.68]	2.20 [1.70;2.92]	< 0.001
TIC Type			< 0.001
Type I	6 (2.40 %)	10 (6.58 %)	
Type II	80 (32.00 %)	76 (50.00 %)	
Type III	164 (65.60 %)	66 (43.42 %)	
Position:			0.980
Left	125 (50.00 %)	75 (49.34 %)	
Right	125 (50.00 %)	77 (50.66 %)	
Estrogen receptor state			0.171
Negative	71 (28.40 %)	33 (21.71 %)	
Positive	179 (71.60 %)	119 (78.29 %)	
Progesterone receptor state			0.544
Negative	91 (36.40 %)	50 (32.89 %)	
Positive	159 (63.60 %)	102 (67.11 %)	
HER2 state			< 0.001
HER2-zero	95 (38.00 %)	38 (25.00 %)	
HER2-low	82 (32.80 %)	83 (54.61 %)	
HER2-positive	73 (29.20 %)	31 (20.39 %)	
Ki-67			< 0.001
Low (30 %)	177 (70.8 %)	49 (32.20 %)	
High (≥30 %)	73 (29.2 %)	103 (67.80 %)	
ALN metastasis			0.990
Negative	87 (34.80 %)	52 (34.21 %)	
Positive	163 (65.20 %)	100 (65.79 %)	

TIC: time intensity curve; HER2: human epidermal growth factor receptor 2; ALN: axillary lymph node

3.3. Performance of the machine learning radiomics models

For the classification of HER2-positive from HER2-negative, the RF model outperformed the LR (AUC: 0.777 vs. 0.611, $P < 0.001$) and SVM models (AUC: 0.777 vs. 0.702, $P = 0.064$) in the training cohort. This finding was also observed in the validation cohort. The RF model yielded the highest AUC (0.765), followed by the LR (AUC: 0.542, < 0.001) and SVM models (AUC: 0.714, $P = 0.261$). The performance of each model for task 1 is listed in Table 2. The ROC curve analysis of the radiomics models is shown in Fig. 4. The AUC of the RF model for distinguishing between HER2-low and HER2-zero in the training and validation cohorts were 0.731 and 0.713, respectively, which were higher than those of the other two models. Fig. 5 shows the ROC curve analysis for the identification of the HER2-low status. The discrimination performance of each model is summarized in Table 3. The DCA results demonstrated that the RF algorithm achieved higher net benefits than the other classifiers, with threshold range of 0.125–0.961 for task 1 and 0.205–0.823 for task 2.

4. Discussion

Given the increasing interest in HER2-low in breast carcinoma, we developed machine learning radiomics models based on multisequence MR images for the noninvasive assessment of HER2 status, including HER2-positive, HER2-low, and HER2-zero in IDC. The LR, RF, and SVM classification algorithms were used to build the prediction models. Our results demonstrated that the RF model yielded the best performance in the training cohort. Results were validated using an independent, external validation cohort.

Radiomics is a non-invasively approach that allows the extraction of a multitude of quantitative features from medical images, enabling the delineation of intrinsic biological characteristics. Previous studies have demonstrated the utility of radiomics for classifying of HER2-positive and HER2-negative in breast carcinoma. Li et al. [18] reported that a radiomics model based on MR images for predicting HER2-positive breast carcinoma yielded an AUC of 0.808 in the training cohort. Another study non-invasively evaluated the efficacy of radiomics model based on multiparametric MRI and showed its ability to predict the HER2 status, with an AUC of 0.810 in the validation cohort [26]. In our study, the results revealed an AUC of 0.777 for the RF model for predicting HER2-positive in IDC. These findings are partially consistent with those of above studies, which also showed that machine learning radiomics from multisequence MRI was a useful analytical tool to for identification of HER2-positive IDC.

Recently, a new nomenclature for HER2-low breast carcinomas was proposed. HER2-low breast carcinoma has been actively investigated by both oncologists and pathologists because of its distinct clinical and mutational features compared with HER2-zero and HER2-positive breast cancer. Therefore, the categorization of HER2 into three subtypes: (1) HER2-positive, (2) HER2-low, and (3) HER2-zero, may provide clearer insight into the prognosis and management of IDC patients. Herein, we developed a machine learning radiomics model based on multisequence MRI for the prediction of HER2-low IDC. Four optimal texture features, grey-level cooccurrence matrix, grey-level run-length matrix, and grey-level size zone matrix, were retained to establish a model for distinguishing HER2-low from HER2-zero IDC. According to the hypothesis, texture features are conducive to the better exploration of intratumor heterogeneity and subtle differences in gray and texture level features [27]. In comparison to HER2-zero, the values of these features were significantly higher in the HER2-low group, suggesting more homogeneity in IDC with HER2-low.

In machine learning, classification is considered as a supervised learning task that infers a function from labeled training data [28]. In this study, we employed three classifiers, LR, RF, and SVM, with a

Table 2
Performance of radiomics models with LR, RF, and SVM for task 1.

	AUC (95 % CI)	ACC (95 % CI)	SEN (95 % CI)	SPE (95 % CI)	PPV (95 % CI)	NPV (95 % CI)
Training cohort						
LR	0.611(0.536–0.685)	0.516(0.452–0.579)	0.822(0.643–0.904)	0.390(0.237–0.475)	0.357(0.303–0.379)	0.841(0.763–0.866)
RF	0.777(0.715–0.839)	0.608(0.544–0.669)	0.904(0.741–0.974)	0.486(0.328–0.559)	0.420(0.373–0.439)	0.925(0.892–0.934)
SVM	0.702(0.632–0.772)	0.648(0.585–0.707)	0.781(0.589–0.863)	0.593(0.310–0.678)	0.442(0.374–0.467)	0.868(0.774–0.882)
Validation cohort						
LR	0.542(0.423–0.661)	0.414(0.335–0.497)	0.806(0.484–0.903)	0.314(0.091–0.430)	0.231(0.153–0.252)	0.864(0.647–0.897)
RF	0.765(0.669–0.861)	0.750(0.673–0.817)	0.710(0.452–0.852)	0.760(0.562–0.866)	0.431(0.326–0.477)	0.911(0.883–0.921)
SVM	0.714(0.604–0.825)	0.743(0.666–0.811)	0.581(0.387–0.742)	0.785(0.438–0.909)	0.409(0.316–0.469)	0.880(0.803–0.894)

AUC: area under curve; ACC: accuracy; SEN: sensitivity; SPE: specificity; PPV: positive predict value; NPV: negative predict value; 95 % CI: 95 % confidence interval; LR: logistic regression; RF: random forest; SVM: support vector machine

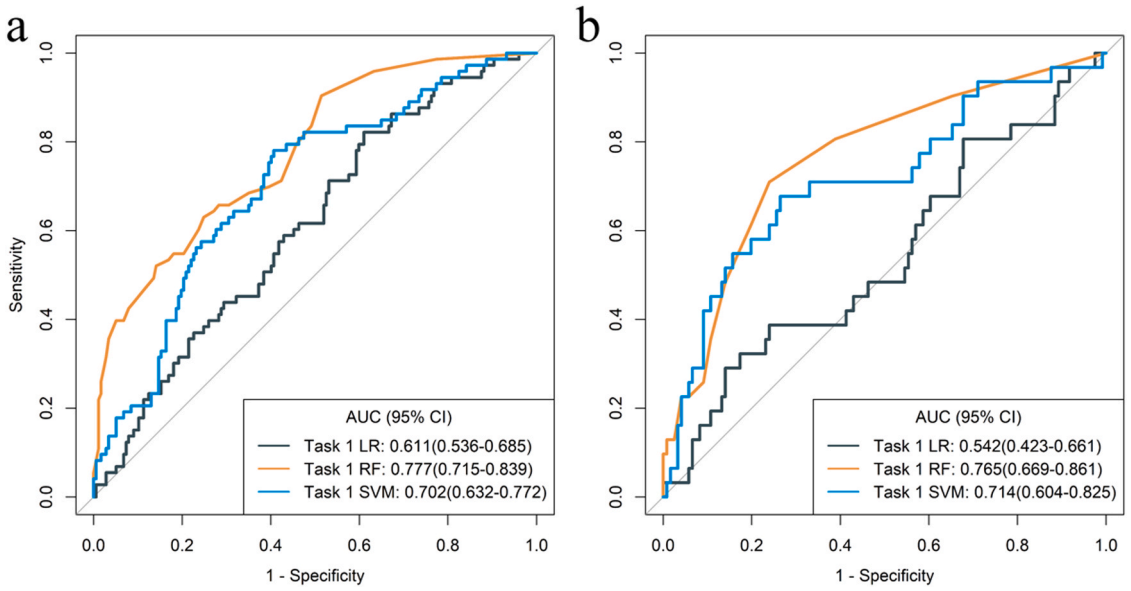

Fig. 4. Areas under the ROC curve of the logistic regression (LR), random forest (RF), and support vector machine (SVM) classifiers in the classification of HER2-positive from HER2-negative in the training cohort (a) and validation cohort (b).

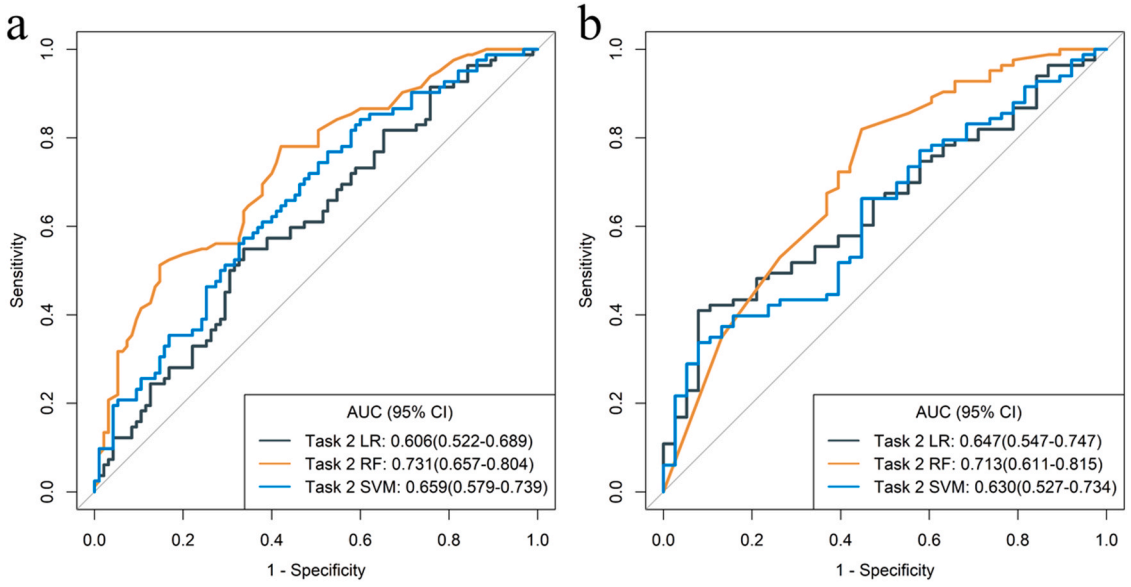

Fig. 5. Areas under the ROC curve of the logistic regression (LR), random forest (RF), and support vector machine (SVM) classifiers in the classification of HER2-low and HER2-zero in the training cohort (a) and validation cohort (b).

Table 3
Performance of radiomics models with LR, RF, and SVM for task 2.

	AUC (95 % CI)	ACC (95 % CI)	SEN (95 % CI)	SPE (95 % CI)	PPV (95 % CI)	NPV (95 % CI)
Training cohort						
LR	0.606(0.522–0.689)	0.610(0.534–0.682)	0.549(0.305–0.634)	0.663(0.442–0.758)	0.584(0.439–0.619)	0.630(0.532–0.661)
RF	0.731(0.657–0.804)	0.695(0.621–0.762)	0.512(0.354–0.626)	0.853(0.626–0.918)	0.750(0.674–0.786)	0.669(0.598–0.686)
SVM	0.659(0.579–0.739)	0.610(0.534–0.682)	0.768(0.634–0.878)	0.474(0.305–0.611)	0.558(0.510–0.590)	0.703(0.604–0.753)
Validation cohort						
LR	0.647(0.547–0.747)	0.562(0.469–0.652)	0.518(0.421–0.723)	0.658(0.447–0.895)	0.768(0.729–0.822)	0.385(0.298–0.459)
RF	0.713(0.611–0.815)	0.727(0.639–0.804)	0.964(0.892–1.000)	0.211(0.078–0.421)	0.727(0.712–0.735)	0.727(0.498–0.842)
SVM	0.630(0.527–0.734)	0.653(0.561–0.737)	0.855(0.783–0.976)	0.211(0.079–0.448)	0.703(0.684–0.730)	0.400(0.200–0.587)

AUC: area under curve; ACC: accuracy; SEN: sensitivity; SPE: specificity; PPV: positive predict value; NPV: negative predict value; 95 % CI: 95 % confidence interval; LR: logistic regression; RF: random forest; SVM: support vector machine

relatively large number of samples to obtain more accurate results. Our results demonstrated the AUC of RF was higher than those of LR and SVM for HER2 status prediction in the training cohort, and this was verified by the multicenter dataset. RF is a widely used machine learning algorithm with many important advantages, such as an effective structure for complex multimodal data and parallel computing [29]. Yu et al. [30] developed an MRI-based RF model to predict the axillary lymph node metastasis status and disease-free interval in breast cancer and provided useful clinical decision-making guidance. Zhang et al. [31] reported an XGBoost model based on the ultrasound signs to predict sentinel lymph node metastasis. Based on the above data, the machine learning radiomics could be a convenient preoperative approach for assessing molecular subtypes in patients with IDC.

This study had several limitations. First, its retrospective design may have introduced a selection bias. Additional studies are needed to further validate the diagnostic performance of the models established using a large cohort. Second, manually delineated ROIs were used. In a future study, we will employ the semiautomatic and automatic ROI methods. Third, only primary IDC lesions were included. The validation of the results of relapsed lesions is also crucial in clinical practice.

5. Conclusions

Machine learning-based multisequence MRI radiomics features can effectively classify IDC patients into groups based on their HER2 expression status. This provides supplementary information to clinicians for precise medical interventions in patients with IDC.

Funding

This research is supported by the Applied Basic Research Programs of Shanxi Province (grant number 20210302123290).

Ethical statement

This retrospective study was approved by ethics committees of Second Hospital of Shanxi Medical University (number: 2023YXD293) and the Third Affiliated Hospital of Zunyi Medical University (number: 2022-1-26), which waived the requirement for informed consent. All methods were performed in accordance with the Declaration of Helsinki.

CRediT authorship contribution statement

Xiao-Li Song: Writing – review & editing, Writing – original draft, Supervision, Project administration, Methodology, Investigation, Conceptualization. **Jin liang Niu:** Writing – review & editing, Supervision, Methodology, Investigation, Formal analysis, Conceptualization. **Li mei Guo:** Writing – original draft, Software, Methodology, Formal analysis, Data curation. **Jia-Liang Ren:** Writing – review & editing, Writing – original draft, Visualization, Validation, Software, Methodology, Investigation, Formal analysis, Data curation. **Hong-Jian Luo:** Writing – review & editing, Writing – original draft, Visualization, Software, Project administration, Methodology, Investigation, Formal analysis, Data curation, Conceptualization.

Declaration of Competing Interest

The authors declare that they have no known competing financial interests or personal relationships that could have appeared to influence the work reported in this paper.

Appendix A. Supporting information

Supplementary data associated with this article can be found in the online version at doi:10.1016/j.ejro.2024.100592.

References

[1] H. Sung, J. Ferlay, R.L. Siegel, M. Laversanne, I. Soerjomataram, A. Jemal, F. Bray, Global cancer statistics 2020: GLOBOCAN estimates of incidence and mortality worldwide for 36 cancers in 185 countries, CA Cancer J. Clin. 71 (3) (2021) 209–249.
[2] E. Hamilton, M. Shastry, S.M. Shiller, R. Ren, Targeting HER2 heterogeneity in breast cancer, Cancer Treat. Rev. 100 (2021) 102286.
[3] A.C. Wolff, M.E.H. Hammond, K.H. Allison, B.E. Harvey, P.B. Mangu, J.M. S. Bartlett, M. Bilous, I.O. Ellis, P. Fitzgibbons, W. Hanna, R.B. Jenkins, M.F. Press, P.A. Spears, G.H. Vance, G. Viale, L.M. McShane, M. Dowsett, Human epidermal growth factor receptor 2 testing in breast cancer: American Society of Clinical Oncology/College of American Pathologists Clinical Practice Guideline Focused Update, J. Clin. Oncol. 36 (20) (2018) 2105–2122.
[4] N. Harbeck, F. Penault-Llorca, J. Cortes, M. Gnant, N. Houssami, P. Poortmans, K. Ruddy, J. Tsang, F. Cardoso, Breast cancer, Nat. Rev. Dis. Prim. 5 (1) (2019) 66.
[5] A.G. Waks, E.P. Winer, Breast cancer treatment: a review, Jama 321 (3) (2019) 288–300.
[6] P. Tarantino, E. Hamilton, S.M. Tolaney, J. Cortes, S. Morganti, E. Ferraro, A. Marra, G. Viale, D. Trapani, F. Cardoso, F. Penault-Llorca, G. Viale, F. Andrè, G. Curigliano, HER2-low breast cancer: pathological and clinical landscape, J. Clin. Oncol. 38 (17) (2020) 1951–1962.
[7] C. Denkert, F. Seither, A. Schneeweiss, T. Link, J.U. Blohmer, M. Just, P. Wimberger, A. Forberger, H. Tesch, C. Jackisch, S. Schmatloch, M. Reinisch, E. F. Solomayer, W.D. Schmitt, C. Hanusch, P.A. Fasching, K. Lübbe, C. Solbach, J. Huober, K. Rhiem, F. Marmé, T. Reimer, M. Schmidt, B.V. Sinn, W. Janni, E. Stickeler, L. Michel, O. Stötzer, E. Hahnen, J. Furlanetto, S. Seiler, V. Nekljudova, M. Untch, S. Loibl, Clinical and molecular characteristics of HER2-low-positive breast cancer: pooled analysis of individual patient data from four prospective, neoadjuvant clinical trials, Lancet Oncol. 22 (8) (2021) 1151–1161.
[8] U. Banerji, C.M.L. van Herpen, C. Saura, F. Thistlethwaite, S. Lord, V. Moreno, I. R. Macpherson, V. Boni, C. Rolfo, E.G.E. de Vries, S. Rottey, J. Geenen, F. Eskens, M. Gil-Martin, E.C. Mommers, N.P. Koper, P. Aftimos, Trastuzumab duocarmazine in locally advanced and metastatic solid tumours and HER2-expressing breast cancer: a phase 1 dose-escalation and dose-expansion study, Lancet Oncol. 20 (8) (2019) 1124–1135.
[9] S. Modi, H. Park, R.K. Murthy, H. Iwata, K. Tamura, J. Tsurutani, A. Moreno-Aspitia, T. Doi, Y. Sagara, C. Redfern, I.E. Krop, C. Lee, Y. Fujisaki, M. Sugihara, L. Zhang, J. Shahidi, S. Takahashi, Antitumor activity and safety of trastuzumab Deruxtecan in patients with HER2-low-expressing advanced breast cancer: results from a phase Ib study, J. Clin. Oncol. 38 (17) (2020) 1887–1896.
[10] C. von Arx, P. De Placido, A. Caltavituro, R. Di Rienzo, R. Buonaiuto, M. De Laurentiis, G. Arpino, F. Puglisi, M. Giuliano, L. Del Mastro, The evolving therapeutic landscape of trastuzumab-drug conjugates: future perspectives beyond HER2-positive breast cancer, Cancer Treat. Rev. 113 (2023) 102500.
[11] T. D'Alfonso, Y.F. Liu, S. Monni, P.P. Rosen, S.J. Shin, Accurately assessing her-2/neu status in needle core biopsies of breast cancer patients in the era of neoadjuvant therapy: emerging questions and considerations addressed, Am. J. Surg. Pathol. 34 (4) (2010) 575–581.

[12] F. Miglietta, G. Griguolo, M. Bottosso, T. Giarratano, M. Lo Mele, M. Fassan, M. Cacciatore, E. Genovesi, D. De Bartolo, G. Vernaci, O. Amato, F. Porra, P. Conte, V. Guarneri, M.V. Dieci, HER2-low-positive breast cancer: evolution from primary tumor to residual disease after neoadjuvant treatment, NPJ Breast Cancer 8 (1) (2022) 66.
[13] M.E. Mayerhoefer, A. Materka, G. Langs, I. Häggström, P. Szczypiński, P. Gibbs, G. Cook, Introduction to radiomics, J. Nucl. Med 61 (4) (2020) 488–495.
[14] A. Tahmassebi, G.J. Wengert, T.H. Helbich, Z. Bago-Horvath, S. Alaei, R. Bartsch, P. Dubsky, P. Baltzer, P. Clauser, P. Kapetas, E.A. Morris, A. Meyer-Baese, K. Pinker, Impact of machine learning with multiparametric magnetic resonance imaging of the breast for early prediction of response to neoadjuvant chemotherapy and survival outcomes in breast cancer patients, Invest Radiol. 54 (2) (2019) 110–117.
[15] H. Li, Y. Zhu, E.S. Burnside, K. Drukker, K.A. Hoadley, C. Fan, S.D. Conzen, G. J. Whitman, E.J. Sutton, J.M. Net, M. Ganott, E. Huang, E.A. Morris, C.M. Perou, Y. Ji, M.L. Giger, MR Imaging Radiomics Signatures for Predicting the Risk of Breast Cancer Recurrence as Given by Research Versions of MammaPrint, Oncotype DX, and PAM50 Gene Assays, Radiology 281 (2) (2016) 382–391.
[16] K. Drukker, H. Li, N. Antropova, A. Edwards, J. Papaioannou, M.L. Giger, Most-enhancing tumor volume by MRI radiomics predicts recurrence-free survival "early on" in neoadjuvant treatment of breast cancer, Cancer Imaging 18 (1) (2018) 12.
[17] D. Leithner, M.E. Mayerhoefer, D.F. Martinez, M.S. Jochelson, E.A. Morris, S. B. Thakur, K. Pinker, Non-invasive assessment of breast cancer molecular subtypes with multiparametric magnetic resonance imaging radiomics, J. Clin. Med. 9 (6) (2020).
[18] C. Li, L. Song, J. Yin, Intratumoral and peritumoral radiomics based on functional parametric maps from breast DCE-MRI for prediction of HER-2 and Ki-67 status, J. Magn. Reson Imaging 54 (3) (2021) 703–714.
[19] C. Fang, J. Zhang, J. Li, H. Shang, K. Li, T. Jiao, D. Yin, F. Li, Y. Cui, Q. Zeng, Clinical-radiomics nomogram for identifying HER2 status in patients with breast cancer: a multicenter study, Front. Oncol. 12 (2022) 922185.
[20] T. Fujii, T. Kogawa, W. Dong, A.A. Sahin, S. Moulder, J.K. Litton, D. Tripathy, T. Iwamoto, K.K. Hunt, L. Pusztai, B. Lim, Y. Shen, N.T. Ueno, Revisiting the definition of estrogen receptor positivity in HER2-negative primary breast cancer, Ann. Oncol. 28 (10) (2017) 2420–2428.
[21] T.O. Nielsen, S.C.Y. Leung, D.L. Rimm, A. Dodson, B. Acs, S. Badve, C. Denkert, M. J. Ellis, S. Fineberg, M. Flowers, H.H. Kreipe, A.V. Laenkholm, H. Pan, F. M. Penault-Llorca, M.Y. Polley, R. Salgado, I.E. Smith, T. Sugie, J.M.S. Bartlett, L. M. McShane, M. Dowsett, D.F. Hayes, Assessment of Ki67 in breast cancer: updated recommendations from the international Ki67 in breast cancer working group, J. Natl. Cancer Inst. 113 (7) (2021) 808–819.
[22] J.J.M. van Griethuysen, A. Fedorov, C. Parmar, A. Hosny, N. Aucoin, V. Narayan, R.G.H. Beets-Tan, J.C. Fillion-Robin, S. Pieper, H. Aerts, Computational radiomics system to decode the radiographic phenotype, Cancer Res. 77 (21) (2017) e104–e107.
[23] A. Zwanenburg, M. Vallières, M.A. Abdalah, H. Aerts, V. Andrearczyk, A. Apte, S. Ashrafinia, S. Bakas, R.J. Beukinga, R. Boellaard, M. Bogowicz, L. Boldrini, I. Buvat, G.J.R. Cook, C. Davatzikos, A. Depeursinge, M.C. Desseroit, N. Dinapoli, C.V. Dinh, S. Echegaray, I. El Naqa, A.Y. Fedorov, R. Gatta, R.J. Gillies, V. Goh, M. Götz, M. Guckenberger, S.M. Ha, M. Hatt, F. Isensee, P. Lambin, S. Leger, R.T. H. Leijenaar, J. Lenkowicz, F. Lippert, A. Losnegård, K.H. Maier-Hein, O. Morin, H. Müller, S. Napel, C. Nioche, F. Orlhac, S. Pati, E.A.G. Pfaehler, A. Rahmim, A.U. K. Rao, J. Scherer, M.M. Siddique, N.M. Sijtsema, J. Socarras Fernandez, E. Spezi, R. Steenbakkers, S. Tanadini-Lang, D. Thorwarth, E.G.C. Troost, T. Upadhaya, V. Valentini, L.V. van Dijk, J. van Griethuysen, F.H.P. van Velden, P. Whybra, C. Richter, S. Löck, The image biomarker standardization initiative: standardized quantitative radiomics for high-throughput image-based phenotyping, Radiology 295 (2) (2020) 328–338.
[24] C. Blüthgen, M. Patella, A. Euler, B. Baessler, K. Martini, J. von Spiczak, D. Schneiter, I. Opitz, T. Frauenfelder, Computed tomography radiomics for the prediction of thymic epithelial tumor histology, TNM stage and myasthenia gravis, PLoS One 16 (12) (2021) e0261401.
[25] R.A. Rutenbar, Simulated annealing algorithms: an overview, IEEE Circuits Devices 5 (1) (1989) 19–26.
[26] J. Zhou, H. Tan, W. Li, Z. Liu, Y. Wu, Y. Bai, F. Fu, X. Jia, A. Feng, H. Liu, M. Wang, Radiomics signatures based on multiparametric MRI for the preoperative prediction of the HER2 status of patients with breast cancer, Acad. Radiol. 28 (10) (2021) 1352–1360.
[27] S.A. Waugh, C.A. Purdie, L.B. Jordan, S. Vinnicombe, R.A. Lerski, P. Martin, A. M. Thompson, Magnetic resonance imaging texture analysis classification of primary breast cancer, Eur. Radiol. 26 (2) (2016) 322–330.
[28] B. Mao, L. Zhang, P. Ning, F. Ding, F. Wu, G. Lu, Y. Geng, J. Ma, Preoperative prediction for pathological grade of hepatocellular carcinoma via machine learning-based radiomics, Eur. Radiol. 30 (12) (2020) 6924–6932.
[29] J.M. Nguyen, P. Jézéquel, P. Gillois, L. Silva, F. Ben Azzouz, S. Lambert-Lacroix, P. Juin, M. Campone, A. Gaultier, A. Moreau-Gaudry, D. Antonioli, Random forest of perfect trees: concept, performance, applications and perspectives, Bioinformatics 37 (15) (2021) 2165–2174.
[30] Y. Yu, Y. Tan, C. Xie, Q. Hu, J. Ouyang, Y. Chen, Y. Gu, A. Li, N. Lu, Z. He, Y. Yang, K. Chen, J. Ma, C. Li, M. Ma, X. Li, R. Zhang, H. Zhong, Q. Ou, Y. Zhang, Y. He, G. Li, Z. Wu, F. Su, E. Song, H. Yao, Development and validation of a preoperative magnetic resonance imaging radiomics-based signature to predict axillary lymph node metastasis and disease-free survival in patients with early-stage breast cancer, JAMA Netw. Open 3 (12) (2020) e2028086.
[31] G. Zhang, Y. Shi, P. Yin, F. Liu, Y. Fang, X. Li, Q. Zhang, Z. Zhang, A machine learning model based on ultrasound image features to assess the risk of sentinel lymph node metastasis in breast cancer patients: applications of scikit-learn and SHAP, Front Oncol. 12 (2022) 944569.